Original Article

Quantification of volumetric thigh and paravertebral muscle fat content: comparison of quantitative Dixon (Q-Dixon) magnetic resonance imaging (MRI) with high-speed T_2-corrected multiecho MR spectroscopy

Wenshuang Zhang[1#^], Chen Fu[2#], Dong Yan[3], Yi Yuan[1,3], Wei Zhang[3], Dalong Gu[3], Yanglei Wu[4], Dongliang Zhang[2], Ling Wang[3,5^], Xiaoguang Cheng[1,3]

[1]Department of Radiology, Peking University Fourth School of Clinical Medicine, Beijing, China; [2]Department of Nephrology, National Center for Orthopaedics, Beijing Jishuitan Hospital, Capital Medical University, Beijing, China; [3]Department of Radiology, National Center for Orthopaedics, Beijing Jishuitan Hospital, Capital Medical University, Beijing, China; [4]MR Research Collaboration, Siemens Healthineers, Beijing, China; [5]JST Sarcopenia Research Centre, National Center for Orthopaedics, Beijing Research Institute of Traumatology and Orthopaedics, Beijing Jishuitan Hospital, Capital Medical University, Beijing, China

Contributions: (I) Conception and design: L Wang, Wenshuang Zhang; (II) Administrative support: L Wang, X Cheng; (III) Provision of study materials or patients: D Zhang, D Yan; (IV) Collection and assembly of data: C Fu, Y Yuan, W Zhang, D Gu; (V) Data analysis and interpretation: W Zhang; (VI) Manuscript writing: All authors; (VII) Final approval of manuscript: All authors.

[#]These authors contributed equally to this work.

Correspondence to: Xiaoguang Cheng, PhD, MD. Department of Radiology, Peking University Fourth School of Clinical Medicine, No. 31, Xinjiekou East Street, Beijing 100035, China; Department of Radiology, National Center for Orthopaedics, Beijing Jishuitan Hospital, Capital Medical University, No. 31, Xinjiekou East Street, Beijing 100035, China. Email: xiao65@263.net; Ling Wang, PhD, MD. Department of Radiology, National Center for Orthopaedics, Beijing Jishuitan Hospital, Capital Medical University, No. 31, Xinjiekou East Street, Beijing 100035, China; JST Sarcopenia Research Centre, National Center for Orthopaedics, Beijing Research Institute of Traumatology and Orthopaedics, Beijing Jishuitan Hospital, Capital Medical University, Beijing, China. Email: doctorwl@bjmu.edu.cn; Dongliang Zhang, MD. Department of Nephrology, National Center for Orthopaedics, Beijing Jishuitan Hospital, Capital Medical University, No. 31, Xinjiekou East Street, Beijing 100035, China. Email: zhangdongliang@jst-hosp.com.cn.

Background: Muscle fat infiltration (MFI) is increasingly recognized as a critical factor influencing muscle function and metabolic health. Accurate quantification of MFI is essential for diagnosing and monitoring various muscular and metabolic disorders. Quantitative Dixon (Q-Dixon) magnetic resonance imaging (MRI) and high-speed T_2-corrected multi-echo (HISTO) magnetic resonance spectroscopy (MRS) are both advanced imaging techniques that offer potential for detailed assessment of MFI. However, the validity and reliability of these methods in measuring volumetric changes in muscle composition, particularly in both thigh and paravertebral muscles, have not been thoroughly compared. This study aims to validate volumetric measurements using Q-Dixon MRI against HISTO MRS in thigh and paravertebral muscles, taking into account the heterogeneity of MFI.

Methods: A retrospective study was conducted with 54 subjects [mean age, 60 years; 38 male (M)/16 female (F)] for thigh muscle and 56 subjects (mean age, 50 years; 22 M/34 F) for paravertebral muscle assessment using a 3-Tesla MRI. The proton density fat fraction (PDFF) was measured with Q-Dixon MRI and HISTO MRS within the upper-middle part of quadriceps femoris and paravertebral muscles at L4/5 level in

^ ORCID: Wenshuang Zhang, 0000-0002-9291-2538; Ling Wang, 0000-0002-5129-4999.

volumes-of-interest (VOIs). The corresponding volumetric Q-Dixon freehand VOI PDFF was measured. Scatterplots, Bland-Altman plots, Spearman correlation coefficients, and Wilcoxon signed rank test with Bonferroni correction were employed. The Kruskal-Wallis *H* tests followed by Bonferroni-corrected post hoc tests were analyzed to compare parameter differences with visual MFI grades.

Results: Q-Dixon cubic VOI PDFF correlated positively with HISTO MRS PDFF in thigh (r=0.96, P<0.001) and paravertebral groups (r=0.98, P<0.001), with insignificant differences (P=0.29, 0.82, respectively). Both PDFF values from cubic VOIs in Q-Dixon and HISTO MRS differed from the freehand Q-Dixon PDFF (all P<0.001). Only for <5% HISTO MRS PDFF, there was a difference between HISTO MRS PDFF and Q-Dixon cubic VOI PDFF (P=0.002).

Conclusions: Volumetric Q-Dixon cubic VOI PDFF exhibited good correlation and consistency with HISTO MRS PDFF for quantitative fat assessment in thigh and paravertebral muscles except for muscles with fat fraction <5%, and the Q-Dixon freehand VOI PDFF offers a more comprehensive assessment of the actual MFI compared to cubic VOI.

Keywords: Magnetic resonance imaging (MRI); magnetic resonance spectroscopy (MRS); muscle; fat quantification

Submitted Jan 21, 2024. Accepted for publication Apr 26, 2024. Published online Jun 13, 2024.
doi: 10.21037/qims-24-127
View this article at: https://dx.doi.org/10.21037/qims-24-127

Introduction

Muscle fat infiltration (MFI) is an essential aspect of muscle health that directly influences muscle strength and functionality (1,2). Its relevance spans several metabolic and musculoskeletal disorders, including chronic kidney disease (3), type 2 diabetes (4,5), chronic pain (6-8), sarcopenia (9), and muscular dystrophy (10,11). MFI occurs both at a macroscopic level called intermuscular adipose tissue (IMAT), either as perimuscular adipose tissue accumulated between muscle groups or as intramuscular adipose tissue inside muscles called extramyocellular lipids (EMCL), and at a microscopic level inside myocytes called intramyocellular lipids (IMCL) (12,13). MFI could distort muscle architecture, further resulting in negative impacts on muscular function (14). The complex interplay between MFI and muscle loss contributes to reduced mobility, vulnerability to fragility fractures, and other detrimental health outcomes (15-19). Consequently, accurate and reliable quantification of muscle fat content is indispensable for clinical practice and research.

Magnetic resonance imaging (MRI) has emerged as the primary modality to evaluate MFI (11,20). One is water-fat separation based and another is proton magnetic resonance spectroscopy (^{1}H MRS) based. Various MRI techniques, commonly recognized in the field as quantitative Dixon (Q-Dixon) (21) for water-fat separation and high-speed T_2-corrected multi-echo (HISTO) (22) for ^{1}H MRS respectively, facilitate noninvasive reproducible examination and quantitative measurement of fat proportion in the liver (22,23), bone (21), bone marrow (24) and muscle (25,26). Both methods quantify volumetric tissue fat in terms of proton density fat fraction (PDFF), defined as the ratio of the signal strength from fat to the total signal from fat and water (27,28). ^{1}H MRS is considered the reference standard for non-invasive quantification of fat content in vivo, both in liver (29,30) and muscle (25,26). Compared with T_1-weighted (T_1w) imaging without the capability of detecting IMCL (31), HISTO MRS, and Q-Dixon MRI have greater accuracy and objectivity for quantifying the total muscle fat content (IMAT and IMCL) (25). Both methods show advantages in MFI quantitative assessment, especially for a fat content of 50% or less with lipids mainly stored as IMCL which are not visually identified as fat in traditional MRI. However, the cubic volume-of-interest (VOI) with a small volume of HISTO MRS restricts its clinical applications. Q-Dixon MRI provides scalable maps of fat distribution, which may be more representative of the overall muscle fat distribution (32), and the VOIs for volumetric fat quantification can be placed in any size and location after image acquisition, which makes the Q-Dixon MRI much more realistically achievable for clinical routine and for quantification in clinical research.

Only a few studies have looked into the relationship

between HISTO MRS and the cross-sectional region-of-interest (ROI) based measurements of Q-Dixon MRI which focused on areal PDFF measurements predominantly (25,26). To date, there are no dedicated reports about the comparison of volumetric PDFF measurements between HISTO MRS and Q-Dixon MRI, specifically in the context of thigh and paravertebral muscle fat content. The use of volumetric measurements even combined with the freehand delineation can provide a more comprehensive understanding of the spatial distribution of fat within the muscles, which necessitates a more extensive exploration and validation of volumetric PDFF measurements via Q-Dixon MRI.

The primary objective of this study is to validate the accuracy of volumetric Q-Dixon cubic VOI PDFF for quantifying the fat content in thigh and paravertebral muscles, using HISTO MRS PDFF as the reference standard. In addition, we aim to highlight the enhanced clinical applicability of volumetric Q-Dixon freehand VOI PDFF compared to cubic VOI PDFF. Ultimately, our research aspires to solidify the role of volumetric Q-Dixon PDFF as an essential tool in radiology, thereby facilitating more comprehensive and robust assessments of MFI. We present this article in accordance with the STROBE reporting checklist (available at https://qims.amegroups.com/article/view/10.21037/qims-24-127/rc).

Methods

Study population

This study was a retrospective analysis of prospectively collected data, which was conducted according to the principles of the Declaration of Helsinki (as revised in 2013) and in accordance with the current scientific guidelines. The study protocol was approved by the institutional ethics committee of Beijing Jishuitan Hospital (No. 202112-11-01). Written informed consent was obtained from each subject prior to examination.

One hundred and ten adults were recruited from February 2022 to August 2023 in Beijing Jishuitan Hospital. Of these, the thigh muscles of only 54 subjects were measured (thigh muscle group), while the paravertebral muscles of the remaining 56 subjects were measured (paravertebral muscle group). The age of participants was widely distributed between 19 and 89 years. Inclusion criteria were adults more than 18 years old with complaints of back pain, muscle weakness, or limited mobility warranting an MRI evaluation of the thigh or lumbar region in Beijing Jishuitan Hospital. Exclusion criteria were pregnant women, individuals with pacemakers or certain metal implants; or people who had a history of surgical or invasive procedures in the thigh or lumbar region within the past year; or individuals who were intolerant of MRI examination because of claustrophobia or psychiatric conditions. No subjects were excluded based on the above criteria (*Figure 1*).

Magnetic resonance examination

Magnetic resonance examination was performed on a 3-Tesla MR system (MAGNETOM Vida, Siemens Healthcare, Erlangen, Germany), with a flexible 18-channel body radiofrequency surface coil for the thigh and a phased-array spine coil for lumbar paravertebral muscles in supine position with headfirst towards the MR system. Apart from the Q-Dixon MRI and HISTO MRS protocol, a conventional clinically common T_1w turbo spin echo (TSE) sequence for high-resolution anatomical reference was obtained. All detailed imaging parameters are summarized in *Table 1*.

Images of the left thigh quadriceps femoris (from the proximal border of the patella to the superior aspect of the femoral lesser trochanter) or lumbar paravertebral muscles were obtained in both Q-Dixon MRI and T_1w TSE sequence. Quadriceps femoris in the thigh and the paravertebral muscles in the L4/L5 intervertebral level were chosen because both of them could be separated well from surrounding muscles or tissues and were large enough to encompass the entire HISTO MRS VOI (20×20×20 mm^3 for paravertebral muscle; 30×30×30 mm^3 for thigh muscle) in all subjects.

HISTO MRS protocol and MRS measurement

The spectroscopy method for quantitative muscle fat measurement was a single-voxel HISTO MRS sequence, which was performed in the stimulated echo acquisition mode (STEAM) and could quantify lipid percentages by correcting for the R_2 relaxation of water and fat (22). The reconstructed axial, coronal, and sagittal planes of T_1w images were used to guide the localization of the left mid-thigh quadriceps femoris or the left paravertebral muscles in L4/L5 intervertebral level with the HISTO MRS VOI placement. The HISTO MRS VOI was positioned on three-planes reconstructed from the T_1w localizing

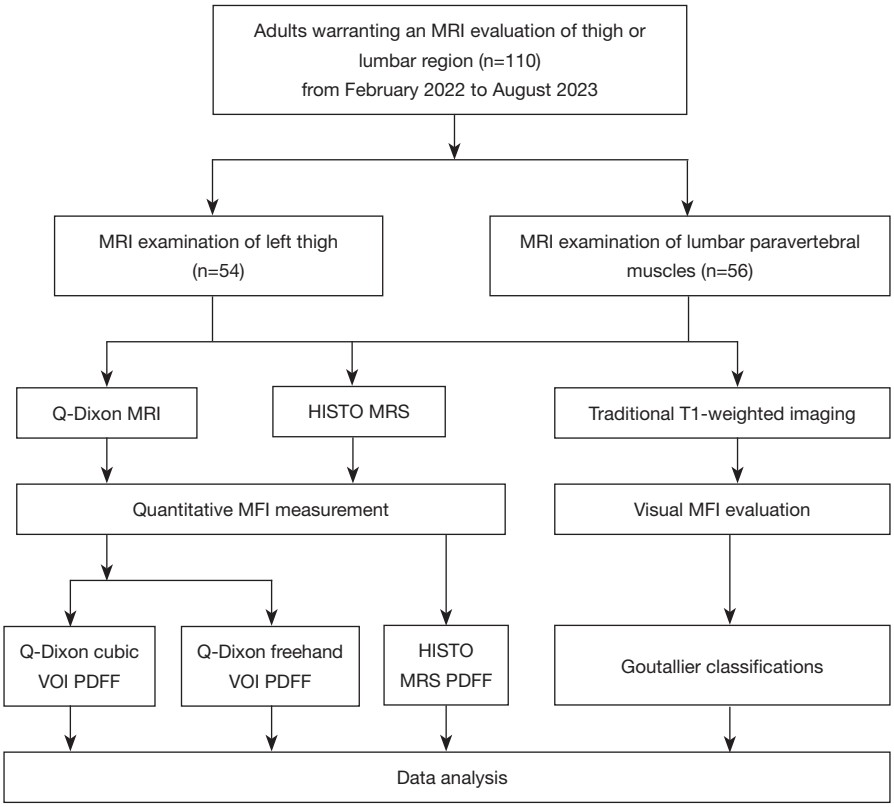

Figure 1 Flowchart summarizes the study design. MRI, magnetic resonance imaging; Q-Dixon, quantitative Dixon; HISTO, high-speed T_2-corrected multi-echo; MRS, magnetic resonance spectroscopy; MFI, muscle fat infiltration; VOI, volume-of-interest; PDFF, proton density fat fraction.

Table 1 Imaging parameters of MRI protocol

Sequence	T_1w TSE	HISTO MRS	Q-Dixon MRI
TR (msec)	3.88	3,000	8.82
TE (msec)	2.46	12/24/36/48/72	1.05/2.46/3.69/4.92/6.15/7.38
TM (msec)	–	10	–
Spatial resolution (mm^3)	1.4×1.4×3.0	–	1.4×1.4×3.0
HISTO MRS VOI size (mm^3)	–	20×20×20 or 30×30×30[a]	–
Slice thickness (mm)	3.0	–	3.0
Slices	104	–	104
FOV (mm^2)	450×390	–	450×390
FA (°)	–	90	4
BW (Hz/px)	1,042	1,200	1,080
NA	1	1	1
TA (min:sec)	0:12	0:15	0:17

[a], the size of HISTO MRS VOI is 20×20×20 mm^3 for paravertebral muscle and 30×30×30 mm^3 for thigh muscle. MRI, magnetic resonance imaging; T_1w, T_1-weighted; TSE, turbo spin echo; HISTO, high speed T_2-corrected multi-echo; MRS, magnetic resonance spectroscopy; Q-Dixon, quantitative Dixon; TR, repetition time; TE, echo time; TM, mixing time; VOI, volume-of-interest; FOV, field of view; FA, flip angle; BW, bandwidth; NA, number of acquisitions; TA, acquisition time.

images, avoiding the main vessels and femoral bone by the MR technologist at the time of the HISTO MRS scan. Additionally, the dimensions of the HISTO MRS VOI were specified as 20×20×20 mm^3 for the left paravertebral muscles and 30×30×30 mm^3 for the left thigh muscles. The rationale behind this differentiation is that thigh muscles, being generally bulkier, are more accurately represented with a 30×30×30 mm^3 cubic VOI for optimal PDFF analysis. However, the paravertebral muscles, being thinner, necessitate a smaller VOI of 20×20×20 mm^3 to avoid including areas beyond the muscle boundaries.

The HISTO MRS VOI was placed in the upper-middle part of the quadriceps femoris without macroscopic fatty septa, if possible. Additionally, the HISTO MRS VOI could not exceed the outer edges of the quadriceps femoris in the axial, coronal, and sagittal planes. The center of the HISTO MRS cubic VOI was located in the quadriceps femoris starting at approximately 8 cm below the lower border of the lesser trochanter. The basic placement principle for the HISTO MRS VOI within paravertebral muscles in L4/L5 level aligns with the method described in the prior paragraph. The positioning of the HISTO MRS VOI is visualized in *Figure 2*. Following the completion of the HISTO MRS sequence scan, the HISTO MRS PDFF value was automatically generated.

Q-Dixon MRI protocol and MRI measurement

The Q-Dixon MRI is a multi-echo three-dimensional (3D) gradient echo (GRE) volumetric interpolated breath-hold examination (VIBE) T_2*-corrected 6-point (6pt) Q-Dixon sequence, which is used to generate water, fat, T_2*, R_2*, in-phase and opposed-phase images (31). Finally, PDFF map reconstruction could be automatically completed. Reconstructed PDFF maps of the Q-Dixon sequence were processed with open-source software ITK-SNAP (version 3.6) (33) for the data extraction.

To compare fat measurements between the Q-Dixon and HISTO MRS sequence, the locations of Q-Dixon MRI cubic VOIs were manually placed in the same position on the quadriceps femoris or lumbar paravertebral muscles using the axial, coronal, and sagittal planes for the same participant as far as possible according to precise spatial coordinates of HISTO MRS cubic VOIs (*Figure 2*). The VOIs—20 mm cubic for paravertebral muscles and 30 mm cubic for thigh muscles—were manually positioned on the Q-Dixon PDFF images.

On Q-Dixon MRI, the volumetric PDFF, derived from freehand segmentation of left side of the quadriceps or the left paravertebral muscles (inclusive of the erector spinae and multifidus, along with the intermuscular fascia), was also evaluated. This type of freehand-delineated VOI is termed Q-Dixon freehand VOI, with the corresponding PDFF referred to as Q-Dixon freehand VOI PDFF. The freehand VOI was delineated on each 3 mm thick axial slice, spanning 10 slices for the thigh muscle and 7 slices for the paravertebral muscle. The central slice was positioned approximately 8 cm below the lower border of the lesser trochanter (Figure S1), ensuring the entirety of the HISTO MRS VOI was encompassed within the selected slices (*Figure 2*).

All the Q-Dixon MRI cubic VOI placement and freehand segmentations were measured by two radiologists (Reader 1 and Reader 2) respectively to determine the interobserver precision, who were blinded to HISTO MRS PDFF results and each other's findings. For each VOI, the values measured independently by two readers were averaged to obtain a final value, which was then used for statistical analysis. This approach was consistently applied to both the Q-Dixon cubic VOI PDFF and the Q-Dixon freehand VOI PDFF. Repeated measurements were performed in a randomly selected group comprising 15 subjects each from both the thigh and paravertebral groups, totaling 30 subjects, to assess the intraobserver variability by one reader (Reader 1) after a six-week internal on the Q-Dixon PDFF images.

Visual MFI evaluation in T_1w imaging

The T_1w MR images were independently graded based on a Goutallier classification (34) by two radiologists (Reader 1, with 6 years of experience; and Reader 2, with 5 years of experience) as grade 0 (G0, no fatty streaks), grade 1 (G1, some fatty streaks), grade 2 (G2, more muscle than fat), grade 3 (G3, as much fat as muscle) and grade 4 (G4, less muscle than fat). Any disagreement was resolved by discussion and consensus including a third more experienced reader (Reader 3, with 12 years of experience). The final agreed classifications were formulated and available for further analysis.

Statistical analysis

Statistical analysis was performed by using the SPSS software (version 26, IBM Corp. Armonk, NY, USA) and GraphPad Prism (Version 7.04, GraphPad Software

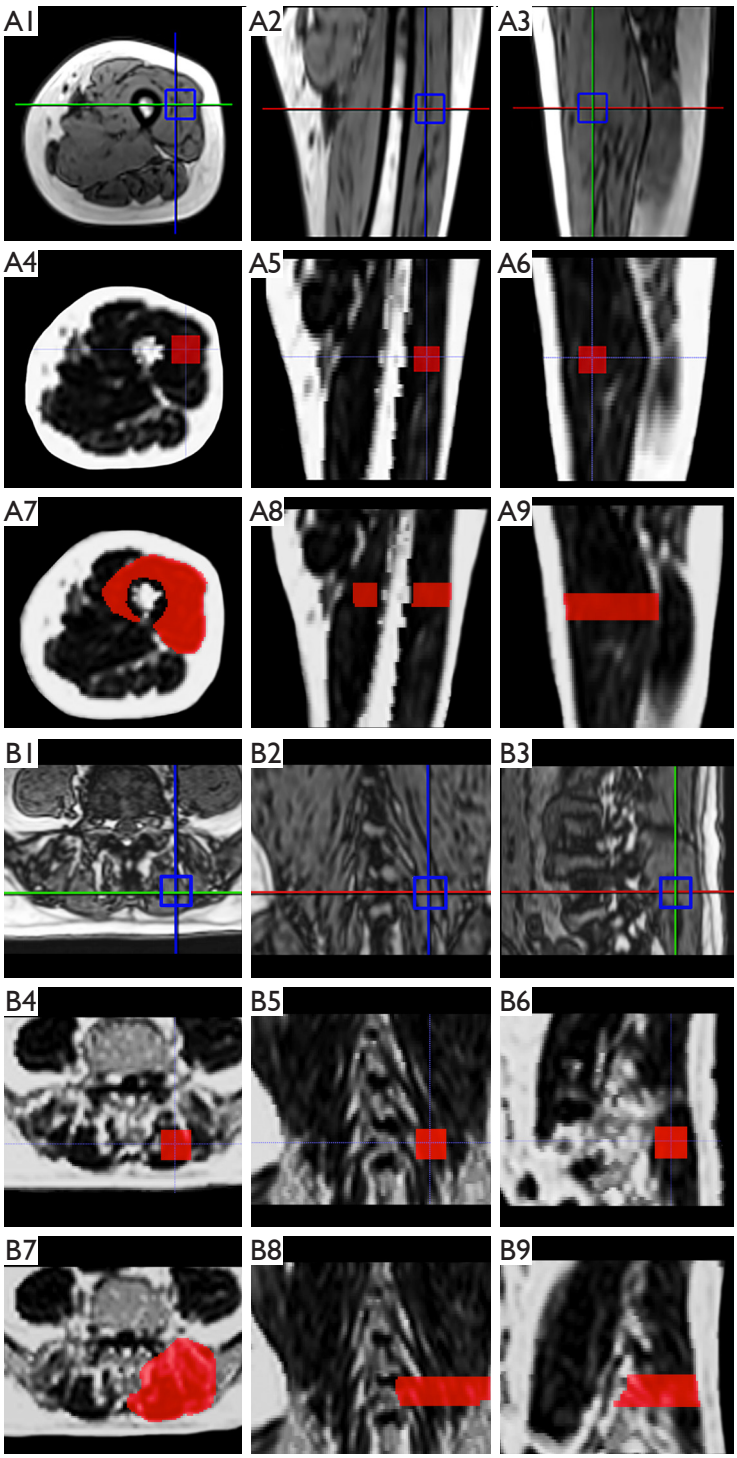

Figure 2 Localization diagrams for VOI measurements of left quadriceps femoris and left paravertebral muscles fat content on HISTO MRS and Q-Dixon MRI. Axial, coronal, and sagittal images of the left thigh in a 47-year-old woman (A1-A3) and the paravertebral muscles in a 69-year-old man (B1-B3) reconstructed from 3D T_1w images were used for HISTO MRS VOI localization. Matching axial, coronal, and sagittal views from Q-Dixon fat fraction mapping depict Q-Dixon cubic VOI PDFF [(A4-A6) thigh, (B4-B6) paravertebral muscles] and freehand PDFF [(A7-A9) thigh, (B7-B9) paravertebral muscles]. The size of cubic VOI is 30×30×30 mm^3 for thigh muscle (A1-A6) and 20×20×20 mm^3 for paravertebral muscle (B1-B6). VOI, volume-of-interest; HISTO, high-speed T_2-corrected multi-echo; MRS, magnetic resonance spectroscopy; Q-Dixon, quantitative Dixon; MRI, magnetic resonance imaging; 3D, three-dimensional; T_1w, T_1-weighted; PDFF, proton density fat fraction.

Table 2 Characteristics in thigh group and paravertebral muscles group

Parameters	Total	G grades			P value
		0	1	2	
Thigh group					
Sample size (n)	54	8	37	9	–
Age (years)	61.5 (52.2, 68.5)	53.9 (42.6, 67.0)	58.8 (51.8, 67.3)	64.5 (63.9, 78.4)	0.06
Gender (male), n (%)	38 (70.4)	7 (87.5)	28 (75.7)	3 (33.3)	0.23
BMI (kg/m^2)	21.7 (20.1, 25.0)	22.0 (21.3, 24.9)	20.8 (19.7, 24.3)	23.5 (21.0, 27.4)	0.36
HISTO MRS PDFF (%)	6.05 (4.25, 11.91)	2.72 (1.33, 3.80)	5.90 (4.84, 9.54)	18.11 (14.50, 27.03)	<0.001
Q-Dixon cubic VOI PDFF (%)	6.52 (4.44, 11.11)	3.25 (3.02, 3.70)	6.42 (4.92, 8.10)	16.58 (14.87, 24.50)	<0.001
Paravertebral muscles group					
Sample size (n)	56	18	21	17	–
Age (years)	51.4 (37.7, 60.8)	38.2 (29.8, 44.5)	54.5 (42.8, 59.2)	65.2 (53.8, 68.4)	<0.001
Gender (male), n (%)	22 (39.3)	8 (44.4)	8 (38.1)	6 (35.3)	0.85
BMI (kg/m^2)	23.7 (22.6, 26.1)	23.7 (21.5, 24.9)	26.0 (22.7, 27.0)	23.4 (22.6, 26.1)	0.28
HISTO MRS PDFF (%)	9.70 (6.14, 17.32)	4.86 (2.99, 6.14)	9.79 (8.24, 14.51)	20.05 (17.58, 22.06)	<0.001
Q-Dixon cubic VOI PDFF (%)	9.58 (5.61, 17.66)	4.54 (3.48, 5.61)	9.77 (7.93, 14.27)	19.99 (18.08, 21.80)	<0.001

The distribution of characteristics is based on MR classification. Statistical difference analysis is performed between different Goutallier grades by using Chi-square tests for categorical variables and Kruskal-Wallis *H* tests for continuous variables. Continuous variables are presented as medians (25th quartile, 75th quartile). Categorical variables were expressed as numbers and percentages. P<0.05 represents statistically significant. G grades, Goutallier grades; BMI, body mass index; HISTO, high-speed T_2-corrected multi-echo; MRS, magnetic resonance spectroscopy; PDFF, proton density fat fraction; Q-Dixon, quantitative Dixon; VOI, volume-of-interest; MR, magnetic resonance.

Inc.). Continuous variables were expressed as means ± standard deviation or medians (25th quartile, 75th quartile). Categorical variables were expressed as numbers and percentages. The Shapiro-Wilk normality test was used to assess continuous data distribution. Interobserver reliability analysis of visual MFI evaluation in T_1w images between two radiologists (Reader 1 and Reader 2) was performed with weighted Cohen's kappa coefficient (weighted κ values), which were interpreted as follows: 0 (poor), 0–0.20 (slight), 0.21–0.40 (fair), 0.41–0.60 (moderate), 0.61–0.80 (substantial), and 0.81–1.0 (almost perfect agreement) (34). Inter- and intra-observer agreement of quantitative Q-Dixon PDFF results were determined by calculating the intraclass correlation coefficient (ICC), which was interpreted as follows: ≤0.40 (poor), 0.40–0.58 (fair), 0.59–0.75 (good), and >0.75 (excellent) (34). HISTO MRS PDFF and Q-Dixon PDFF measurements were plotted as histograms, and the mean and standard deviation (for normal distribution) or median and interquartile range (for nonnormal distribution) were calculated. Scatterplots, Bland-Altman plots, and Spearman correlation coefficients were used to examine the relationship between HISTO MRS PDFF and Q-Dixon PDFF. The Wilcoxon signed rank test with Bonferroni correction was used for pairwise comparisons between HISTO MRS PDFF, Q-Dixon cubic VOI PDFF, and Q-Dixon freehand VOI PDFF. Furthermore, we also compared the differences between HISTO MRS PDFF and Q-Dixon cubic VOI PDFF in distinct Goutallier grades (G0–G2) groups and in various HISTO MRS fat fraction groups (<5%, 5–9.9%, 10–14.9% and ≥15%), respectively. The Kruskal-Wallis *H* tests followed by Bonferroni-corrected post hoc tests were analyzed to compare quantitative parameter differences with visual MFI-evaluated grades. P values <0.05 were considered to indicate statistical significance.

Results

The characteristics of the thigh and paravertebral muscle groups are detailed separately in *Table 2*. All MR sequences were successfully implemented without technical problems, and detailed MRI data were available for all subjects.

Table 3 Inter- and intraobserver agreement for visual and quantified evaluation

Parameters	Weighted κ/ICC	95% CI	P value
Interobserver agreement			
G grades	0.541[a]	0.408–0.675	<0.001
Q-Dixon cubic VOI PDFF (%)	0.927[b]	0.895–0.949	<0.001
Q-Dixon freehand PDFF (%)	0.908[b]	0.869–0.936	<0.001
Intraobserver agreement			
Q-Dixon cubic VOI PDFF (%)	0.932[b]	0.862–0.967	<0.001
Q-Dixon freehand PDFF (%)	0.912[b]	0.823–0.957	<0.001

[a], interobserver reliability analysis of visual MFI evaluation was performed with weighted κ values; [b], inter- and intraobserver agreement of quantitative Q-Dixon PDFF were determined by ICC. P<0.05 represents statistically significant. Weighted κ, weighted Cohen's kappa coefficient; ICC, intraclass correlation coefficient; CI, confidence interval; G grades, Goutallier grades; Q-Dixon, quantitative Dixon; VOI, volume-of-interest; PDFF, proton density fat fraction.

Interobserver agreement of initial visual MFI evaluations in T_1w images by Reader 1 and Reader 2 was relatively low (*Table 3*). Following consensus, 52.7% (58/110) of participants were classified as Goutallier grade 1, with both grades 0 and 2 representing 23.6% (26/110) each. Additionally, no subjects were classified with a grade of 3 or 4.

Distribution of HISTO MRS PDFF and Q-Dixon cubic VOI PDFF measurements

Figure 3 shows the distributions of the volumetric measurements of HISTO MRS PDFF and Q-Dixon cubic VOI PDFF, respectively, plotted as histograms. The HISTO MRS PDFF ranged from 1.02% to 37.35% for thigh (*Figure 3A*) and 0.59% to 26.45% for paravertebral muscles (*Figure 3E*), compared with 2.08% to 38.39% for thigh (*Figure 3B*) and 1.39% to 24.59% for paravertebral muscles (*Figure 3F*) respectively for the Q-Dixon cubic VOI PDFF measurements. The description of data distribution is detailed in *Table 2*. As a measure of repeatability, both interobserver and intraobserver agreements of quantitative Q-Dixon cubic VOI PDFF were found to be excellent (*Table 3*).

Correlation, Bland-Altman analysis, and comparisons of HISTO MRS and Q-Dixon PDFF measurements

Figure 3 shows the scatterplot and Bland-Altman plot, respectively, of HISTO MRS PDFF against Q-Dixon cubic VOI PDFF. For the 54 thigh muscles (*Figure 3C,3D*), the scatterplot has a positive correlation (r^2=0.96; P<0.001) with an overall bias of –0.04%, and the Bland-Altman plot shows that 96.3% (52/54) of the measured values were within the 95% limit of agreement for HISTO MRS PDFF and Q-Dixon cubic VOI PDFF. For the 56 paravertebral muscles (*Figure 3G,3H*), scatterplots and Bland-Altman plots showing similar outcomes are comprehensively depicted. Wilcoxon signed-ranks test showed that there was statistically no significant difference between HISTO MRS PDFF and Q-Dixon cubic VOI PDFF in MFI quantified measurements of quadriceps femoris (P=0.82) and lumbar paravertebral muscles (P=0.29). However, PDFF values from cubic VOIs in both Q-Dixon MRI and HISTO MRS significantly differed from the volumetric PDFF obtained via freehand delineation on Q-Dixon MRI (all P<0.001; Figure S2).

In different Goutallier grades (G0–G2) groups (*Figure 4*), there was no statistically significant difference between HISTO MRS PDFF and Q-Dixon cubic VOI PDFF, as well as in the 5–9.9%, 10–14.9% and ≥15% HISTO MRS PDFF groups (*Figure 5*). However, in the group of <5% HISTO MRS PDFF (*Figure 5*), the compared Wilcoxon signed-rank test showed that there was a significant statistical difference between HISTO MRS PDFF and Q-Dixon cubic VOI PDFF, which indicates that in cases of minimal MFI (PDFF <5%), the Q-Dixon cubic VOI PDFF measurements lack precision.

Table 2 also shows Kruskal-Wallis *H* and Bonferroni-corrected post hoc tests of cubic VOI PDFF measured by HISTO MRS and Q-Dixon MRI among different Goutallier grades. Cubic VOI PDFFs were statistically different for grades acquired by Q-Dixon MRI (P<0.001) and by HISTO MRS (P<0.001). The results indicate that,

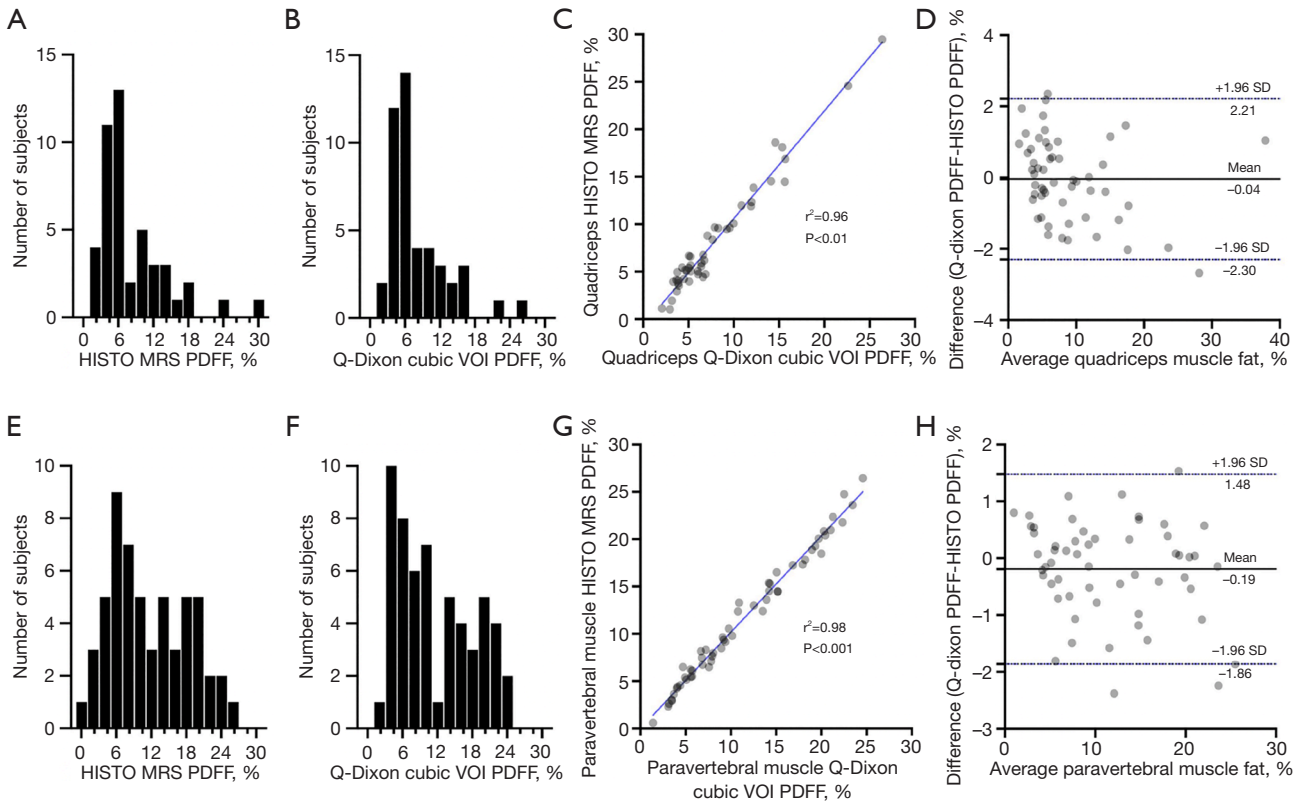

Figure 3 Histograms show measurements of HISTO MRS PDFF and Q-Dixon cubic VOI PDFF for thigh (A,B) and paravertebral muscles (E,F), respectively. Corresponding scatterplots and Bland-Altman plots of quadriceps femoris (C,D) and paravertebral muscles (G,H), respectively. HISTO, high-speed T_2-corrected multi-echo; MRS, magnetic resonance spectroscopy; PDFF, proton density fat fraction; Q-Dixon, quantitative Dixon; VOI, volume-of-interest; SD, standard deviation.

whether for the 54 participants in the thigh group, or the 56 in the paravertebral muscles group, cubic VOI PDFFs determined by Q-Dixon MRI and by HISTO MRS were statistically different among different Goutallier grades (all P<0.001).

Discussion

In the present study, we analyzed the correlation and consistency of cubic volumetric muscle fat content as measured by 6pt Q-Dixon MRI and HISTO MRS in both the thigh and paravertebral muscles. Further, we explored and compared the discrepancies between the freehand segmentation of volumetric Q-Dixon PDFF and the cubic VOI PDFF of either Q-Dixon MRI or HISTO MRS. One of the primary emphases of this research is to underscore the practicality and applicability of volumetric measurements in assessing muscle fat content. Another focal point is to provide data-driven evidence that the volumetric PDFF values measured by Q-Dixon MRI are accurate and reliable. Specifically, in inhomogeneous tissues like muscles, the freehand segmentation of volumetric Q-Dixon PDFF more accurately reflects the true nature of fat infiltration than the cubic VOI PDFF does.

Firstly, our investigation demonstrated that volumetric PDFF measurements obtained using Q-Dixon MRI in cubic VOIs exhibited robust correlation and agreement with HISTO MRS PDFF, which served as the reference standard for quantifying muscle fat content in both the thigh and paravertebral regions. This finding substantiates the reliability and accuracy of Q-Dixon MRI for assessing volumetric MFI. Importantly, using volumetric Q-Dixon freehand VOI PDFF measurements provides a more comprehensive view of muscle fat distribution. This method captures the inherent heterogeneity and subtle variations of fatty infiltration throughout the delineated muscle volume. While areal assessments provide only a snapshot, volumetric evaluations offer a detailed view of the muscle

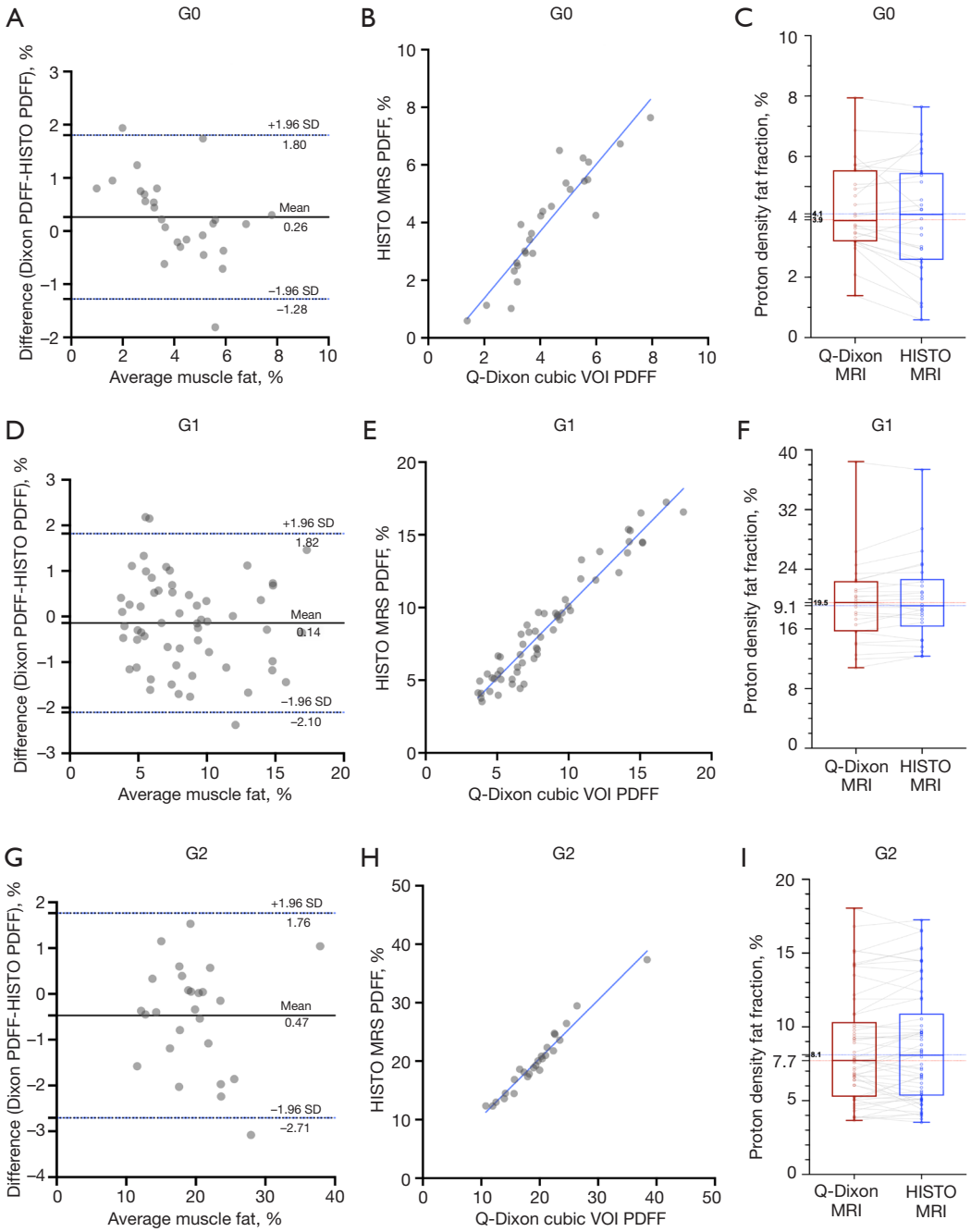

Figure 4 Comparative analysis using scatterplots, Bland-Altman plots, and box plots of HISTO MRS PDFF and Q-Dixon cubic VOI PDFF across Goutallier grades (G0–G2). No significant differences were noted. PDFF, proton density fat fraction; HISTO, high-speed T_2-corrected multi-echo; SD, standard deviation; Q-Dixon, quantitative Dixon; MRI, magnetic resonance imaging; VOI, volume-of-interest; MRS, magnetic resonance spectroscopy; G0, Goutallier grade 0; G2, Goutallier grade 2.

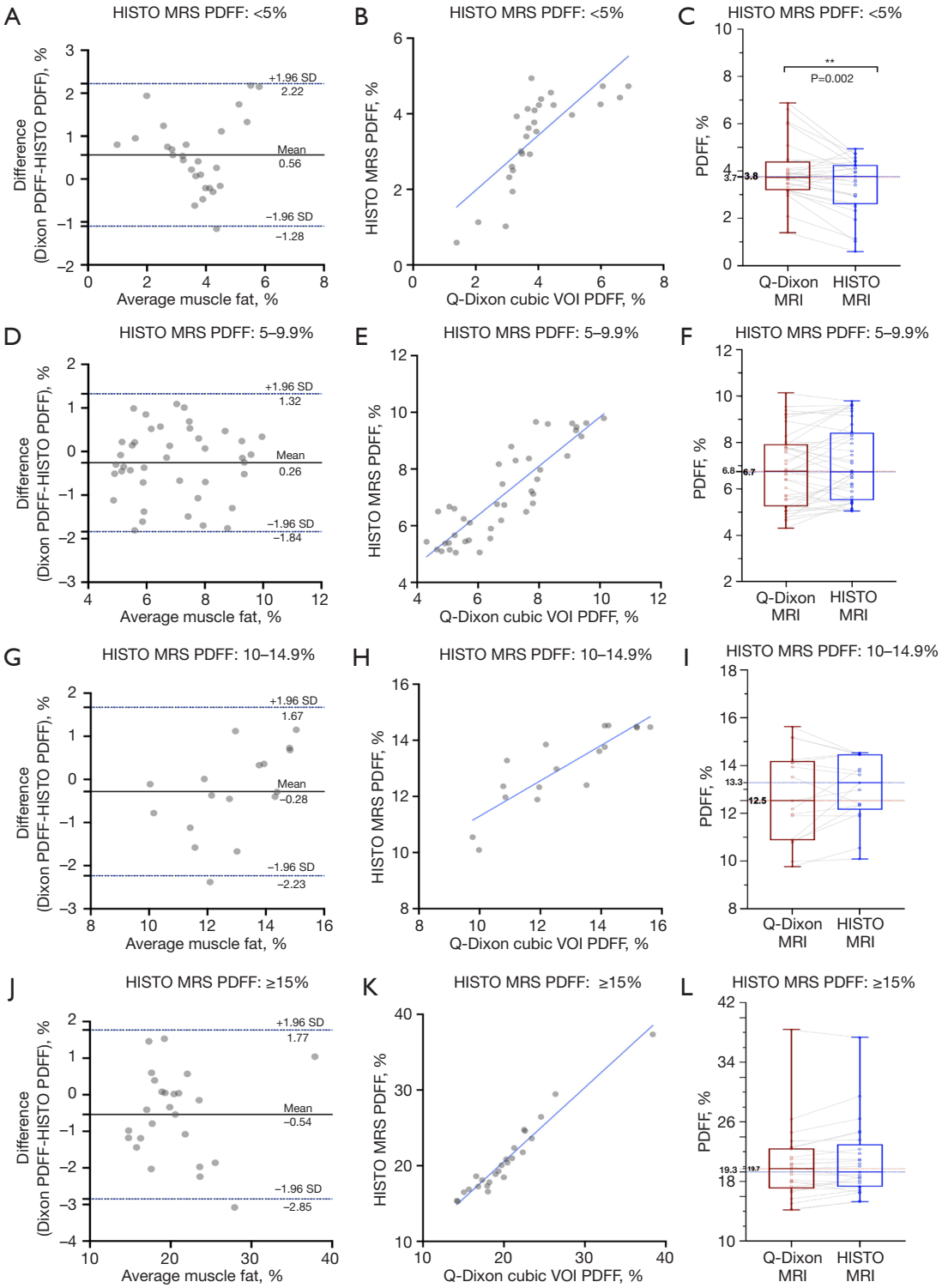

Figure 5 Comparative analysis using scatterplots, Bland-Altman plots, and box plots of HISTO MRS PDFF and Q-Dixon cubic VOI PDFF in the 5–9.9%, 10–14.9% and ≥15% HISTO MRS PDFF groups, respectively. Only in the <5% HISTO MRS PDFF group, a significant statistical discrepancy was observed between HISTO MRS PDFF and Q-Dixon cubic VOI PDFF (P=0.002). **, P<0.01. HISTO, high-speed T_2-corrected multi-echo; MRS, magnetic resonance spectroscopy; PDFF, proton density fat fraction; SD, standard deviation; Q-Dixon, quantitative Dixon; MRI, magnetic resonance imaging; VOI, volume-of-interest.

fat distribution, ensuring a comprehensive representation of fatty infiltration. Our study demonstrates the clinical applicability and potential value of employing volumetric measurements from Q-Dixon MRI in clinical assessments, especially Q-Dixon freehand VOI PDFF measurements.

Secondly, the observed inter- and intraobserver agreement for the volumetric Q-Dixon cubic VOI PDFF was excellent. This outstanding reliability can be largely attributed to the precise process adopted during the delineation of the cubic VOI on Q-Dixon. Given the inherent properties of the sequence, Q-Dixon PDFF map has a relatively lower spatial resolution, leading to suboptimal representation of detailed anatomical structures. Additionally, the coronal, sagittal, and axial positioning of the HISTO MRS VOI during scanning was based on T_1w images. Given these challenges, our study opted to identify the spatial coordinates of the HISTO MRS VOI on the T_1w images first, cross-referencing this with the specific anatomical structure of the muscle. Subsequently, a volumetric mask, mirroring the volume of the HISTO MRS VOI, was delineated on the T_1w images. This mask was then matched to the Q-Dixon PDFF map to derive the corresponding volumetric Q-Dixon cubic VOI PDFF value. This process significantly minimized the potential for subjective measurement errors. Furthermore, our results substantiated that, in terms of inter- and intraobserver agreement, the volumetric Q-Dixon cubic VOI PDFF measurements offered superior reliability compared to the conventional Goutallier classification system used for visual MFI evaluation.

Interestingly, this study observed that in the <5% HISTO MRS PDFF group, there was a significant discrepancy between HISTO MRS PDFF and Q-Dixon cubic VOI PDFF (*Figure 5*). However, no significant differences were found in either the <10% HISTO MRS PDFF group or the 5–9.9% HISTO MRS PDFF group. This suggests that while both methods generally align well, when the muscle fat fraction is less than 5%, the Q-Dixon cubic VOI PDFF shows some deviation compared to the HISTO MRS PDFF. Similar findings have been mentioned in previous studies (25,35). One potential explanation is that in MRI analyses, particularly in low-fat regions, image noise significantly impacts accuracy due to its non-zero mean distribution after magnitude operations, unlike the standard Gaussian distribution with a zero mean. This anomaly, prominent in areas with minimal fat, artificially elevates signal values within the ROI, leading to an overestimation of fat percentages. Therefore, recognizing this noise behavior is crucial for enhancing the precision of fat quantification in MR images, especially in contexts of low-fat fractions.

Additionally, our study demonstrated that the volumetric freehand VOI Q-Dixon PDFF, obtained from delineating one side of the quadriceps and the paravertebral muscles, differed statistically from both the Q-Dixon cubic VOI PDFF and the HISTO MRS PDFF. This result further underscores the limitations of using cubic VOI PDFF for measuring fat content in inhomogeneous tissues like muscle, suggesting that cubic VOI PDFF may not adequately represent the entire muscle due to the inhomogeneity of fatty infiltration. Grimm *et al.* (32) previously reported that the repeatability errors of HISTO MRS VOI PDFF in muscle tissue were pronounced due to the inhomogeneity, elasticity, and susceptibility to deformation of muscle tissue. Furthermore, the viewpoint that cubic VOI MRS is unable to assess the heterogeneity of MFI in skeletal muscle is also recognized in the expert consensus paper (36). Our findings, from the perspective of overall representativeness, resonate with the emphasis on the repeatability of the study by Grimm *et al.*, further collectively emphasizing the clinical practicability of volumetric Q-Dixon freehand VOI PDFF in MFI assessments.

Grimm *et al.* (37) reported the accuracy of 6-point Dixon MRI and MRS in measuring thigh muscle fat, but their study did not involve freehand volumetric PDFF measurements of Q-Dixon MRI. Agten *et al.* (25) confirmed the reliability of the multi-echo Dixon sequence for evaluating early fatty infiltration (within Goutallier grades 0–1) in the supraspinatus muscle, and its results were comparable to MRS. However, their study utilized areal Dixon PDFF in muscles with minimal fat infiltration. The homogeneity of the muscle tissue may lead to the alignment between areal Dixon PDFF and MRS PDFF, limiting its applicability in cases with uneven fat distribution. Our study highlights the significance of volumetric measurements, distinguishing it from the earlier research by Agten *et al.* Our study expands the scope to include evaluation of thigh and paravertebral muscles, covering Goutallier grade 0–2. Additionally, our findings revealed poor agreement between the two observers regarding Goutallier grades. Potential factors that may affect the reliability of Goutallier grading in our study include variations in image quality, differences in interpretation criteria among observers, and the inherent challenges of visually grading MFI, especially in cases with lower fat content. This suggests to some extent that the qualitative assessment method, Goutallier classification,

may not be as precise or robust as quantitative parameters. This conclusion is consistent with the outcomes previously published by our team (38). Overall, the application of volumetric measurements offers a more comprehensive understanding of muscular changes and fat infiltration, especially in cases with inhomogeneous fat distribution. While multiple studies have reported on PDFF accuracy in the liver, in-depth discussions on Dixon PDFF in the muscle domain remain limited (22,23,39).

To the best of our knowledge, no prior studies have emphasized the volumetric measurements of Q-Dixon PDFF in the paravertebral muscles. Importantly, none have provided empirical evidence demonstrating the practicality, objectivity, and comprehensive representativeness of volumetric Q-Dixon freehand VOI PDFF in evaluating MFI within both thigh and paravertebral muscles, especially in mildly inhomogeneous muscle tissues. Interestingly, the subjects in our study exhibited relatively mild MFI (Goutallier grade 0–2). Notably, even with this mild fat infiltration, significant differences between cubic VOI PDFF and freehand VOI PDFF were observed. This suggests that, in instances of more severe and heterogeneous MFI, the discrepancy between cubic VOI PDFF and the actual overall MFI could be even more pronounced.

This study presented several strengths. Firstly, the thorough spatial registration method between the core positions of the Q-Dixon MRI VOIs and the HISTO MRS VOIs ensured the comparability of Q-Dixon and HISTO MRS PDFF measurements. Secondly, attention was paid to both the cubic VOI and the freehand segmentation corresponding to volumetric Q-Dixon PDFF. Furthermore, these measurements of volumetric PDFF were validated in two distinct anatomical muscle groups, the lower limb muscles, and the paravertebral muscles.

Several limitations of our study deserve consideration. First, the number of participants was limited, and none of the evaluated muscles exhibited severe fat infiltration classified as Goutallier grade 3/4. Second, although manually delineating the VOI by experienced hands took about a minute, the application of Artificial Intelligence for fully automated segmentation and measurement has the potential to significantly boost efficiency (40). Our research team is actively exploring such AI-assisted approaches. Thirdly, the HISTO MRS technique, instead of the biochemical extraction or histopathology was used for reference, which could potentially introduce bias and might have the potential to bias results. However, invasive biopsies for muscle fat evaluation are practically infeasible in clinical settings. Lastly, this investigation primarily compared different MR methodologies and did not delve into clinical correlations. Nonetheless, our study importantly lays the technical groundwork for subsequent research on MRI-based muscle fat quantification and its associations with diverse clinical outcomes.

Conclusions

In summary, volumetric measurements using Q-Dixon cubic VOI PDFF overall exhibited good correlation and consistency with HISTO MRS PDFF considered as the reference standard for quantitative fat assessment in both thigh and paravertebral muscles. Notably, in the context of inhomogeneous muscle tissues, freehand segmentation of volumetric Q-Dixon PDFF provides a more comprehensive reflection of actual MFI compared to cubic VOI PDFF. Therefore, Q-Dixon MRI, focusing on volumetric freehand PDFF, could serve as a reliable alternative to HISTO MRS for the rapid quantification of volumetric fat depositions in muscle for future clinical applications.

Acknowledgments

Funding: This work was supported in part by the National Key Research and Development Program of China (No. 2021YFC2501703), the National Natural Science Foundation of China (Nos. 82371956 and 82371957), Beijing Municipal Health Commission (No. BJRITO-RDP-2024), Beijing Hospitals Authority Clinical Medicine Development of Special Funding Support (No. ZYLX202107), Beijing Physician Scientist Training Project (BJPSTP-2024-08), and Beijing Municipal Public Welfare Development and Reform Pilot Project for Medical Research Institutes (No. JYY2023-8).

Footnote

Reporting Checklist: The authors have completed the STROBE reporting checklist. Available at https://qims.amegroups.com/article/view/10.21037/qims-24-127/rc

Conflicts of Interest: All authors have completed the ICMJE uniform disclosure form (available at https://qims.amegroups.com/article/view/10.21037/qims-24-127/coif). Y.W. is an employee of Siemens Healthineers company.

The other authors have no conflicts of interest to declare.

Ethical Statement: The authors are accountable for all aspects of the work in ensuring that questions related to the accuracy or integrity of any part of the work are appropriately investigated and resolved. The study was conducted in accordance with the Declaration of Helsinki (as revised in 2013). The study was approved by institutional ethics committee of Beijing Jishuitan Hospital (No. 202112-11-01) and informed consent was taken from all the participants.

References

1. Hilton TN, Tuttle LJ, Bohnert KL, Mueller MJ, Sinacore DR. Excessive adipose tissue infiltration in skeletal muscle in individuals with obesity, diabetes mellitus, and peripheral neuropathy: association with performance and function. Phys Ther 2008;88:1336-44.
2. Addison O, Marcus RL, Lastayo PC, Ryan AS. Intermuscular fat: a review of the consequences and causes. Int J Endocrinol 2014;2014:309570.
3. Sabatino A, Cuppari L, Stenvinkel P, Lindholm B, Avesani CM. Sarcopenia in chronic kidney disease: what have we learned so far? J Nephrol 2021;34:1347-72.
4. Sparks LM, Goodpaster BH, Bergman BC. The Metabolic Significance of Intermuscular Adipose Tissue: Is IMAT a Friend or a Foe to Metabolic Health? Diabetes 2021;70:2457-67.
5. Yu F, Fan Y, Sun H, Li T, Dong Y, Pan S. Intermuscular adipose tissue in Type 2 diabetes mellitus: Non-invasive quantitative imaging and clinical implications. Diabetes Res Clin Pract 2022;187:109881.
6. Prasetyo M, Nindita N, Murdana IN, Prihartono J, Setiawan SI. Computed tomography evaluation of fat infiltration ratio of the multifidus muscle in chronic low back pain patients. Eur J Radiol Open 2020;7:100293.
7. Huang Y, Wang L, Zeng X, Chen J, Zhang Z, Jiang Y, Nie L, Cheng X, He B. Association of Paraspinal Muscle CSA and PDFF Measurements With Lumbar Intervertebral Disk Degeneration in Patients With Chronic Low Back Pain. Front Endocrinol (Lausanne) 2022;13:792819.
8. Sollmann N, Bonnheim NB, Joseph GB, Chachad R, Zhou J, Akkaya Z, Pirmoazen AM, Bailey JF, Guo X, Lazar AA, Link TM, Fields AJ, Krug R. Paraspinal Muscle in Chronic Low Back Pain: Comparison Between Standard Parameters and Chemical Shift Encoding-Based Water-Fat MRI. J Magn Reson Imaging 2022;56:1600-8.
9. Cruz-Jentoft AJ, Baeyens JP, Bauer JM, Boirie Y, Cederholm T, Landi F, Martin FC, Michel JP, Rolland Y, Schneider SM, Topinková E, Vandewoude M, Zamboni M; European Working Group on Sarcopenia in Older People. Sarcopenia: European consensus on definition and diagnosis: Report of the European Working Group on Sarcopenia in Older People. Age Ageing 2010;39:412-23.
10. Engelke K, Ghasemikaram M, Chaudry O, Uder M, Nagel AM, Jakob F, Kemmler W. The effect of ageing on fat infiltration of thigh and paraspinal muscles in men. Aging Clin Exp Res 2022;34:2089-98.
11. Burakiewicz J, Sinclair CDJ, Fischer D, Walter GA, Kan HE, Hollingsworth KG. Quantifying fat replacement of muscle by quantitative MRI in muscular dystrophy. J Neurol 2017;264:2053-67.
12. Wronska A, Kmiec Z. Structural and biochemical characteristics of various white adipose tissue depots. Acta Physiol (Oxf) 2012;205:194-208.
13. Engelke K, Museyko O, Wang L, Laredo JD. Quantitative analysis of skeletal muscle by computed tomography imaging-State of the art. J Orthop Translat 2018;15:91-103.
14. Delmonico MJ, Harris TB, Visser M, Park SW, Conroy MB, Velasquez-Mieyer P, Boudreau R, Manini TM, Nevitt M, Newman AB, Goodpaster BH; Health, Aging, and Body. Longitudinal study of muscle strength, quality, and adipose tissue infiltration. Am J Clin Nutr 2009;90:1579-85.
15. Tonkin J, Villarroya F, Puri PL, Vinciguerra M. SIRT1 signaling as potential modulator of skeletal muscle diseases. Curr Opin Pharmacol 2012;12:372-6.
16. Wang L, Yin L, Yang M, Ge Y, Liu Y, Su Y, et al. Muscle density is an independent risk factor of second hip fracture: a prospective cohort study. J Cachexia Sarcopenia Muscle 2022;13:1927-37.
17. Legrand D, Vaes B, Matheï C, Adriaensen W, Van Pottelbergh G, Degryse JM. Muscle strength and physical performance as predictors of mortality, hospitalization, and

disability in the oldest old. J Am Geriatr Soc 2014;62:1030-8.
18. Newman AB, Kupelian V, Visser M, Simonsick EM, Goodpaster BH, Kritchevsky SB, Tylavsky FA, Rubin SM, Harris TB. Strength, but not muscle mass, is associated with mortality in the health, aging and body composition study cohort. J Gerontol A Biol Sci Med Sci 2006;61:72-7.
19. Pavasini R, Guralnik J, Brown JC, di Bari M, Cesari M, Landi F, et al. Short Physical Performance Battery and all-cause mortality: systematic review and meta-analysis. BMC Med 2016;14:215.
20. Sabatino A, D'Alessandro C, Regolisti G, di Mario F, Guglielmi G, Bazzocchi A, Fiaccadori E. Muscle mass assessment in renal disease: the role of imaging techniques. Quant Imaging Med Surg 2020;10:1672-86.
21. Li X, Lu R, Xie Y, Li Q, Tao H, Chen S. Identification of abnormal BMD and osteoporosis in postmenopausal women with T2*-corrected Q-Dixon and reduced-FOV IVIM: correlation with QCT. Eur Radiol 2022;32:4707-17.
22. Pineda N, Sharma P, Xu Q, Hu X, Vos M, Martin DR. Measurement of hepatic lipid: high-speed T2-corrected multiecho acquisition at 1H MR spectroscopy--a rapid and accurate technique. Radiology 2009;252:568-76.
23. Starekova J, Hernando D, Pickhardt PJ, Reeder SB. Quantification of Liver Fat Content with CT and MRI: State of the Art. Radiology 2021;301:250-62.
24. Yuan W, Lei Y, Tang C, Qin F, Wen J, Li C, Ling M, Huang J, Zhang H, Long L. Quantification of bone marrow edema in rheumatoid arthritis by using high-speed T2-corrected multiecho acquisition of (1)H magnetic resonance spectroscopy: a feasibility study. Clin Rheumatol 2021;40:4639-47.
25. Agten CA, Rosskopf AB, Gerber C, Pfirrmann CW. Quantification of early fatty infiltration of the rotator cuff muscles: comparison of multi-echo Dixon with single-voxel MR spectroscopy. Eur Radiol 2016;26:3719-27.
26. Li Z, Zeng H, Han C, Sun L, Fang D, Yu H, Quan X. Effectiveness of High-Speed T2-Corrected Multiecho MR Spectroscopic Method for Quantifying Thigh Muscle Fat Content in Boys With Duchenne Muscular Dystrophy. AJR Am J Roentgenol 2019;212:1354-60.
27. Caussy C, Reeder SB, Sirlin CB, Loomba R. Noninvasive, Quantitative Assessment of Liver Fat by MRI-PDFF as an Endpoint in NASH Trials. Hepatology 2018;68:763-72.
28. Uhrig M, Mueller J, Longerich T, Straub BK, Buschle LR, Schlemmer HP, Mueller S, Ziener CH. Susceptibility based multiparametric quantification of liver disease: Non-invasive evaluation of steatosis and iron overload. Magn Reson Imaging 2019;63:114-22.
29. Reeder SB, Cruite I, Hamilton G, Sirlin CB. Quantitative Assessment of Liver Fat with Magnetic Resonance Imaging and Spectroscopy. J Magn Reson Imaging 2011;34:729-49.
30. Hwang I, Lee JM, Lee KB, Yoon JH, Kiefer B, Han JK, Choi BI. Hepatic steatosis in living liver donor candidates: preoperative assessment by using breath-hold triple-echo MR imaging and 1H MR spectroscopy. Radiology 2014;271:730-8.
31. Grimm A, Meyer H, Nickel MD, Nittka M, Raithel E, Chaudry O, Friedberger A, Uder M, Kemmler W, Quick HH, Engelke K. Evaluation of 2-point, 3-point, and 6-point Dixon magnetic resonance imaging with flexible echo timing for muscle fat quantification. Eur J Radiol 2018;103:57-64.
32. Grimm A, Meyer H, Nickel MD, Nittka M, Raithel E, Chaudry O, Friedberger A, Uder M, Kemmler W, Engelke K, Quick HH. Repeatability of Dixon magnetic resonance imaging and magnetic resonance spectroscopy for quantitative muscle fat assessments in the thigh. J Cachexia Sarcopenia Muscle 2018;9:1093-100.
33. Yushkevich PA, Piven J, Hazlett HC, Smith RG, Ho S, Gee JC, Gerig G. User-guided 3D active contour segmentation of anatomical structures: significantly improved efficiency and reliability. Neuroimage 2006;31:1116-28.
34. Zi Y, Zhang B, Liu L, Cao X, Zeng W, Li X, Zhang G, Wan J, Shi L, Wu H. Fat content in lumbar paravertebral muscles: Quantitative and qualitative analysis using dual-energy CT in correlation to MR imaging. Eur J Radiol 2022;148:110150.
35. Kukuk GM, Hittatiya K, Sprinkart AM, Eggers H, Gieseke J, Block W, Moeller P, Willinek WA, Spengler U, Trebicka J, Fischer HP, Schild HH, Träber F. Comparison between modified Dixon MRI techniques, MR spectroscopic relaxometry, and different histologic quantification methods in the assessment of hepatic steatosis. Eur Radiol 2015;25:2869-79.
36. Kršśák M, Lindeboom L, Schrauwen-Hinderling V, Szczepaniak LS, Derave W, Lundbom J, Befroy D, Schick F, Machann J, Kreis R, Boesch C. Proton magnetic resonance spectroscopy in skeletal muscle: Experts' consensus recommendations. NMR Biomed 2021;34:e4266.
37. Grimm A, Meyer H, Nickel MD, Nittka M, Raithel E, Chaudry O, Friedberger A, Uder M, Kemmler W, Engelke K, Quick HH. A Comparison between 6-point Dixon MRI and MR Spectroscopy to Quantify Muscle Fat in the Thigh of Subjects with Sarcopenia. J Frailty Aging 2019;8:21-6.

38. Zhang W, Ge Y, Liu Y, Yuan Y, Geng J, Zhou F, Huang P, Shi J, Ma K, Cheng Z, Blake GM, Yang M, Wu X, Cheng X, Wang L. Associations of Quantitative and Qualitative Muscle Parameters With Second Hip Fracture Risk in Older Women: A Prospective Cohort Study. JBMR Plus 2023;7:e10834.
39. Bray TJ, Chouhan MD, Punwani S, Bainbridge A, Hall-Craggs MA. Fat fraction mapping using magnetic resonance imaging: insight into pathophysiology. Br J Radiol 2018;91:20170344.
40. Zhang R, He A, Xia W, Su Y, Jian J, Liu Y, Guo Z, Shi W, Zhang Z, He B, Cheng X, Gao X, Liu Y, Wang L. Deep Learning-Based Fully Automated Segmentation of Regional Muscle Volume and Spatial Intermuscular Fat Using CT. Acad Radiol 2023;30:2280-9.

Cite this article as: Zhang W, Fu C, Yan D, Yuan Y, Zhang W, Gu D, Wu Y, Zhang D, Wang L, Cheng X. Quantification of volumetric thigh and paravertebral muscle fat content: comparison of quantitative Dixon (Q-Dixon) magnetic resonance imaging (MRI) with high-speed T_2-corrected multiecho MR spectroscopy. Quant Imaging Med Surg 2024;14(7):4490-4505. doi: 10.21037/qims-24-127

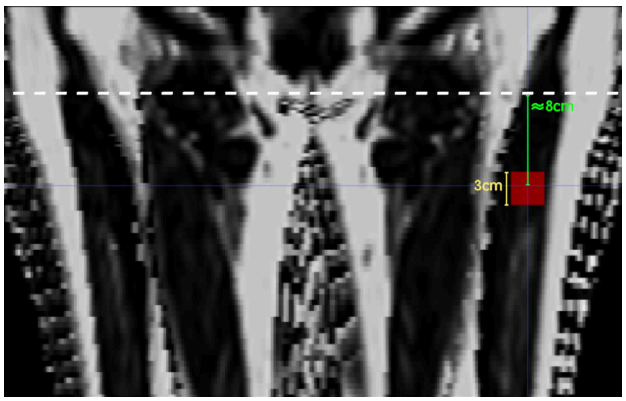

Figure S1 Localization diagrams for 30 mm cubic VOI measurements of the left quadriceps femoris, including the lesser trochanter. The central slice was positioned approximately 8 cm (the length of the green line ≈8 cm) below the lower border of the lesser trochanter (white dashed line). The size of the cubic VOI is 30×30×30 mm^3 (the length of the yellow line =3 cm). The subject depicted in this image is identical to the individual featured in *Figure 2A*. VOI, volume-of-interest.

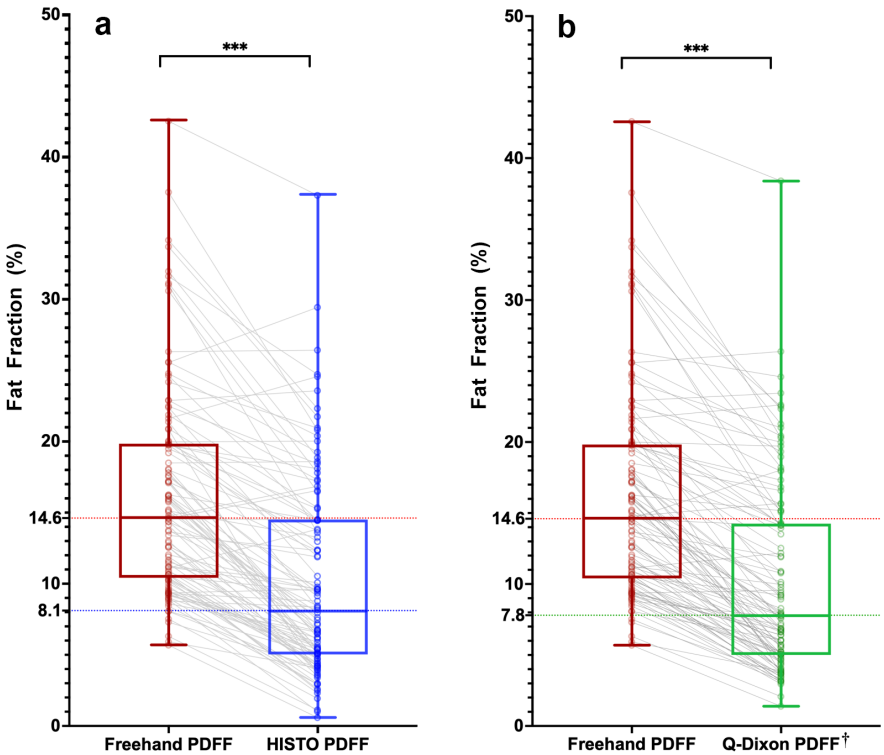

Figure S2 Box plots of PDFF values comparing different measurement techniques. (A) Comparison between Q-Dixon freehand VOI PDFF and HISTO MRS PDFF. (B) Comparison between Q-Dixon freehand VOI PDFF and Q-Dixon cubic VOI PDFF. The Wilcoxon signed-rank test with Bonferroni correction was used to evaluate the differences. †, Q-Dixon cubic VOI PDFF; ***, P<0.001. PDFF, proton density fat fraction; Q-Dixon, quantitative Dixon; VOI, volume-of-interest; HISTO, high-speed T_2-corrected multi-echo; MRS, magnetic resonance spectroscopy.

https://dx.doi.org/10.21037/qims-24-127